PAPER • OPEN ACCESS

Characterization of the wake behind a horizontal-axis wind turbine (HAWT) at very high Reynolds numbers

View the article online for updates and enhancements.

Characterization of the wake behind a horizontal-axis wind turbine (HAWT) at very high Reynolds numbers

Alexander Piqué[1], Mark A. Miller[2], Marcus Hultmark[1]

1. Department of Mechanical and Aerospace Engineering, Princeton University NJ, USA
2. Aerospace Engineering Department, Pennsylvania State University PA, USA

E-mail: `apique@princeton.edu`

Abstract. The wake of a three-bladed horizontal axis wind turbine was studied at aerodynamic conditions similar to what is experienced by commercially available turbines. Field relevant Reynolds numbers and tip speed ratios were obtained through the use of a high-pressure wind tunnel, at relatively low velocities. Measurements of the streamwise velocity were acquired through the use of the novel nano-scale thermal anemometry probe (NSTAP), which yields very high spatial and temporal resolution, enabling unattenuated turbulence measurements. Profiles of the mean velocity and turbulent fluctuations are presented, as they demonstrate important features of the wake development, such as wake recovery and tip vortex evolution. One dimensional energy spectra are also presented to provide details on the dominant flow features present in the wake. Reynolds number invariance is shown for mean velocity deficit and streamwise variance profiles for all downstream positions presented. Downstream evolution of streamwise variance profiles provides insight to the dynamic interactions between the tip and root vortex, such as their eventual coalescence. Spectral analysis show that the near wake flow-structures are dominated by the tip vortex, but that other larger structures are present as well, which may be related to the wake meandering phenomenon.

1. Introduction
The demand for wind energy has grown alongside the increasing global demand for renewable energy. When operating wind farms, one often aims to place the individual turbines as close to each other as possible to reduce cost of infrastructure. However, upstream turbines reduce the momentum and inject turbulence into the inflows of downstream turbines through their wakes, compromising the energy production of the downstream turbines. As such, there is a trade-off between infrastructure costs and energy loss due to such effects. Considering the extreme case of a flow with no turbulence or mixing, the energy density of an n×n turbine wind farm decays as n^{-1} [1]. Realistic wakes entrain momentum from the surrounding fluid to reenergize the wake, a process that is not fully understood and is affected by the flow configuration. A detailed study of these effects, and effects on downstream turbines can aid in the planning of future wind farms, and potentially provide insight on how to design and operate individual turbines to improve collective power output.

The extremely large length scales of modern wind turbine rotors and their wakes make attempts to characterize the underlying fluid mechanics of these large rotary systems very challenging.

Field studies are limited in what can be measured, the resolution of the measurements, and the statistics are often not fully converged. Most wind tunnel studies have been limited to Reynolds numbers that are several orders of magnitude lower than the operating conditions of field turbines. The few experiments that have reached field-realistic Reynolds numbers ($\mathrm{Re_D}=U_\infty \mathrm{D}\ \nu^{-1}$) on the order of 10 million (modern wind turbines can operate at $\mathrm{Re_D}$ as large has 100 million), such as the MEXICO and NREL experiments, have included limited wake studies with limited spatial resolution, or did not include any wake characterization at all [2, 3]. Computational and analytical studies, typically, do not resolve the flow on the blade level or the full turbulence spectrum in the wake, but instead rely on models to capture the effect of the rotor on the surrounding fluid. Considering the lack of data, numerical or experimental, a wind tunnel experiment at full dynamic similarity could provide new insight as to how wind turbine wakes evolve and how they may impact wind turbine and farm performance.

Common themes of past wind turbine wake studies include the characterization of the differences between the near and far wake regions and the evolution of the tip and root vortices. In the near wake the flow is dictated by the geometric features of the turbine and the far wake is the regime where the signatures of those features are less dominant and wake shape is no longer expected to depend heavily on the unique turbine geometry. Downstream turbines in wind farms typically operate in the far wake, to reduce the velocity deficit they experience, and thus the power losses. However, the near wake serves as the initial conditions of the far wake, so its morphology is important as well, as it initializes the complex vortex system that builds the wake [4, 5]. The complex vortical system primarily consists of the tip and root vortices. It is important to understand the evolution of these structures as they are closely linked with mixing and entrainment of high momentum fluid, and thus the wake recovery. A low frequency shedding behavior, known as wake-meandering, has been observed in some field studies [6], as well as in lower Reynolds number wind tunnel studies [7]. A conclusive explanation for the observed wake meandering is still being sought, where some argue that it may be caused by bluff body shedding while others argue that it may be caused by convection due to large scale structures in the atmospheric boundary layer [8].

Evaluation of high Reynolds number wake effects, specifically Reynolds number invariance, is a distinguishing feature of this study. Some previous laboratory studies have identified that wind turbine wake behavior, up to the third moment, are invariant for $\mathrm{Re_D}>9\times10^4$ [9], but others have concluded that the effects of Reynolds number on tip vortex behavior are still unknown [10]. Previous wind tunnel experiments of the same rotor used in these studies identified a strong Reynolds number dependence on the power coefficient, or C_P, curves up to $\mathrm{Re_D}\approx 10^7$ [11]. The same study observed that $\mathrm{Re_D}$ effects were not as evident for the thrust coefficient, or C_T, curves but it is possible that a trend could have been hidden within experimental uncertainty [11]. High C_T, coupled with a high axial induction factor, has been known to lead to the turbulent wake state [12] which has been thought to contribute to a wake contraction observed in a previous PIV study [13]. The unclear impact of high Reynolds numbers on C_T, along with the impact of C_T on wake behavior, warrants a thorough wake characterization of HAWT wakes at high $\mathrm{Re_D}$ and serves as a motivation for the present study. In this work, velocity deficit and streamwise variance profiles are presented along with the power spectral density in the proximity of the tip vortex.

2. Experimental Methodology
Here, a unique data set is presented of wakes behind a wind turbine rotor at very high Reynolds numbers and realistic tip speed ratios. The high Reynolds numbers are achieved using pressurized air, up to 230 bar, which decreases the kinematic viscosity by close to 200 times. This implies that a model tested in these conditions, and at the same tip-speed-ratio, acts as a 200 times larger turbine, if it were tested in atmospheric conditions (and at the same flow

velocity). This is due to the inverse relationship between length scale and kinematic viscosity in the Reynolds number.

2.1. Experimental Setup

The turbine model used in these experiments has a rotor diameter of 20 cm and is based off of the geometry of a Vestas V27 turbine, with a chord length three times larger along the entire span. A full description of the model turbine's geometry performance, including C_P and C_T curves at different Re_D, can be found in [11]. Considering standard atmospheric conditions and a wind speed of 10 m/s, a Vestas V27 turbine would operate with an Re_D of 18×10^6. The High Reynolds number Test Facility (HRTF) at Princeton University can pressurize the working fluid, air, up to 230 bar, while maintaining flow speeds up to 10 m/s. Further, the use of a pressurized wind tunnel enables tests at relevant tip-speed ratios (λ), as the time scales can be kept relatively large. The maximum Reynolds number that can be achieved with the 20 cm rotor in the HRTF facility is $Re_D = 20 \times 10^6$. Therefore, aerodynamic similarity can be achieved between the field and model scales.

After a contraction and a series of flow conditioners, the flow in the test section of the HRTF is uniform with very low levels of free-stream turbulence. As such, the inflow to the turbine for these experiments is not attempting to replicate the inflow of a turbine in the field. However, this study is aimed at investigating the fundamental fluid mechanics, as well as aerodynamic features in wind turbine wakes, and can be considered a canonical turbine wake. Experiments with shear and/or turbulent inflow better represent the conditions a field turbine operates in, but wake features due to the rotor aerodynamic features may be more challenging to separate from wake features caused by the inflow conditions.

2.2. Instrumentation

Streamwise velocity measurements were acquired using nano-scale hot-wire anemometry. When large Reynolds numbers are achieved using high pressure and a relatively small facility, the smallest length scales in the flow are by definition very small. To avoid spatial filtering by the instrumentation, nano-scale hot-wires were used to acquire the velocity data. The nano-scale thermal anemometry probe (NSTAP) is a nano-scale single component hot-wire that is fabricated at Princeton University, using standard micro-eletromechanical system (MEMS) techniques [14]. The NSTAP sensor used had a 100 nm thick platinum sensing element with a length of 60 μm. Due to its small thermal mass, temporal resolution is also significantly increased. Here, the data were sampled at 200 kHz. The NSTAP was operated in constant temperature anemometry mode (CTA) using a Dantec Dynamics Streamline hot-wire system. A custom 4-axis traversing system mounted inside the HRTF test section was used to position the NSTAP at different downstream, spanwise, and azimuthal positions in the wake. For these experiments, measurements were acquired in planes at the turbine hub-height at five different downstream positions (x/D= 0.77, 1.52, 2.02, 3.52, 5.52). Four different Reynolds numbers were investigated (Re_D = 2.7, 3.6, 4.5, and 7.2×10^6) at an average tip speed ratio of λ=5.54. Calibration of the NSTAP was done by moving it outside of the wake of the turbine, and calibrate it against a pitot tube mounted on the traverse, also outside the wake. No corrections have been applied to the presented data.

3. Results

Profiles of mean velocity deficits and streamwise fluctuations, acquired at hub height, are investigated at different downstream positions ($0.77 \leq x/D \leq 5.52$) and different Reynolds numbers ($2.7 \times 10^6 \leq Re_D \leq 7.2 \times 10^6$). Reynolds number invariance, self similarity, and downstream evolution in the mean velocity and streamwise fluctuation profiles were investigated by a comparison of non-dimensional velocity profiles at different downstream positions and Reynolds numbers.
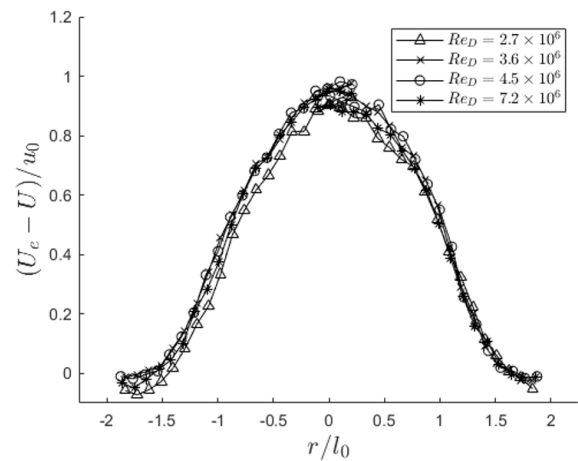
3.1. Mean Velocity Deficit Profiles

Here, the mean velocity deficit is defined as the difference between the mean velocity outside of the wake (U_e) and the mean velocity at a certain radial position in the wake, measured at the same downstream position. In classical wake theory, the mean deficit velocity profile becomes self-similar in the far wake, and at high enough Reynolds numbers it becomes Reynolds number invariant [15]. However, Reynolds number invariance in the turbulence fluctuations has been shown to require significantly higher Reynolds numbers compared to the mean velocity [16], and that a self-similar regime does not appear at all [17] or requires a very large downstream position [18]. For wind turbines, self-similar behavior in the velocity deficit profile has been found to start at 3 diameters downstream [19] whereas the far wake region is taken as 5 diameters downstream [20]. The scaling of the mean and fluctuations are important because they can allow for informed decisions on turbine spacing in wind farms, since the velocity deficit is essentially a measure of the amount of energy that is unavailable to a downstream turbine [21], and the turbulence fluctuations affect the blade fatigue loads and maintenance requirements of a turbine, as well as its performance.

Mean velocity deficit profiles at x/D=0.77 and x/D=5.52 are shown in Figures 1 and 2, where the deficit was nondimensionalized with respect to the deficit velocity (u_0) and the spanwise coordinate is nondimensionalized with respect to the half-width (l_0). The mean velocity profiles for the two downstream locations exhibit distinctively different shapes, implying that they are not self-similar. However, the two do exhibit Reynolds number invariance at their respective locations for the Re_D range that has been tested. Figure 2 shows that the wake is exhibiting a near Gaussian profile, a profile that has been used instead of the top-hat profile in an attempt to improve actuator disk predictions [19]. However, Figure 1 suggests that the velocity profile shape in the near-wake is more complicated and cannot be represented well by a Gaussian profile.
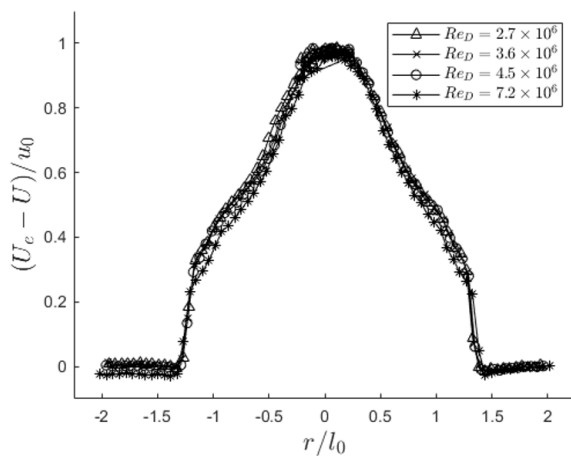

**Figure 1.** Velocity deficit profile at x/D=0.77 for $2.7 \times 10^6 < Re_D < 7.2 \times 10^6$.

Figure 2. Velocity deficit profile at x/D=5.52 for $2.7 \times 10^6 < Re_D < 7.2 \times 10^6$.

Mean velocity deficit profiles at different downstream positions, for Re_D of 2.7×10^6 and 7.2×10^6, are shown in Figures 3 and 4, respectively. These plots are non-dimensionalized with respect to U_e and the turbine diameter, D, such that the wake recovery can be better visualized. As one would expect, the velocity deficit profile decreases in magnitude as the downstream distance increases, regardless of Re_D. As has been noted in previous analytical and experimental studies, wake growth tends to be underestimated due to confinement effects [22, 23, 24]. Considering the rotor swept area, the model turbine's blockage ratio would be approximately 16.66%, large

enough to be affected by confinement effects [22]. Therefore, it is difficult to make a quantitative conclusion on the wake growth from these experiments since blockage corrections were not applied to the presented results. However, the results can still serve as important high Reynolds number reference cases for modelling and numerical simulation efforts, as long as the blockage effects are accurately taken into account.
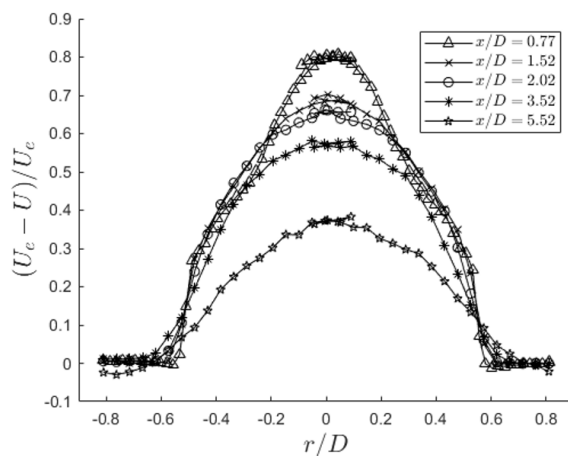
Figure 3. Velocity deficit profile evolution at Re_D=2.7×10^6 for 0.77<x/D<5.52.
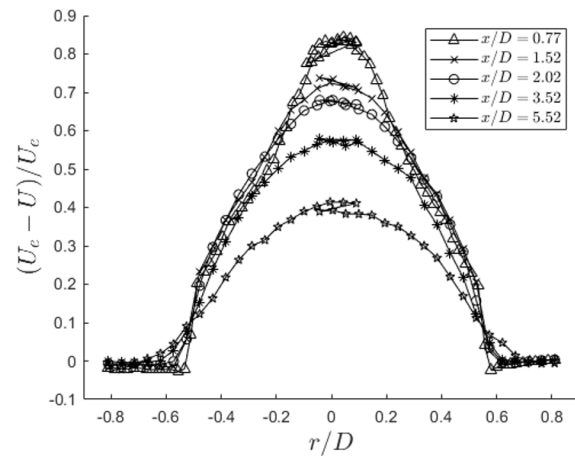
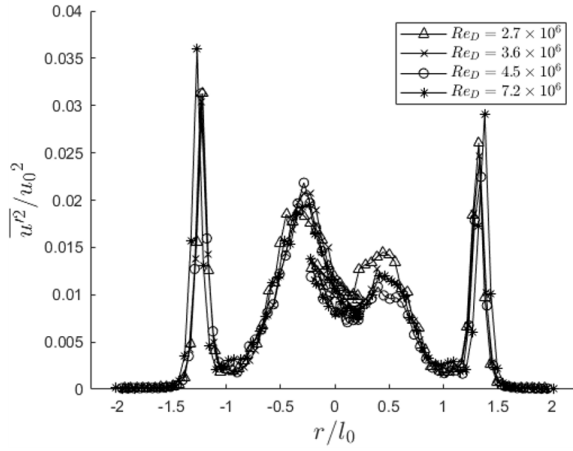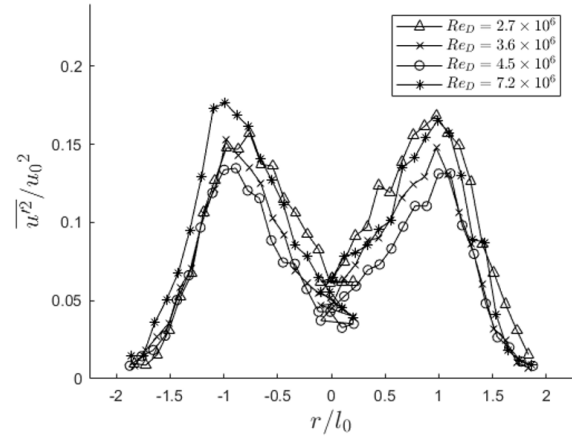**Figure 4.** Velocity deficit profile evolution at Re_D=7.2×10^6 for 0.77<x/D<5.52.

3.2. Streamwise Variance Profiles

Measurements of the turbulence fluctuations provide further information about the scaling of the wake, as well as the turbulent mixing in the wake. Intense mixing regions are expected to be centered about the locations of the tip and root vortices. Variance profiles are presented in a similar fashion as the velocity deficit profiles, so that conclusions on self-similarity, downstream evolution, and Reynolds number invariance can be made.

Trends with Reynolds number in the streamwise fluctuations are shown in Figures 5 and 6 for the closest and farthest downstream positions tested, respectively. Similar to what was observed in the mean velocity deficit profiles, the streamwise fluctuation profiles for the two downstream locations have distinctively different shapes, indicating lack of self-similar behavior this far upstream. Regarding the variance profile at x/D=0.77, Reynolds number invariance is observed for all tested Reynolds numbers, whereas for the farther downstream position (x/D=5.52), conclusions on Reynolds number invariance are not as clear. The shapes of the variance profiles change rapidly as the wake evolves downstream. Close to the rotor it has a distinct four-peak profile which evolves into a two peak profile further downstream. In the near wake, there are two groups of maxima observed in the variance profile, with one pair located near the edge of the wake and another pair located towards the center. The freestream can be identified by the flow region with the smallest amount of velocity variance. At the wake edge there is a large maximum in the streamwise variance which coincides approximately with the tip vortex locations. These sharp peaks are most likely indicators that the helical tip vortex has not become unstable yet, and is still well defined. The concentrated nature of the tip vortex in the near wake has been observed for a similar downstream distance in a previous work [25]. The pair of variance peaks near the center are likely indicators of the root vortex. Their magnitudes are smaller and appear more blunt in their shape, suggesting that the root vortex is weaker than the tip vortex, as has been noted before [4].
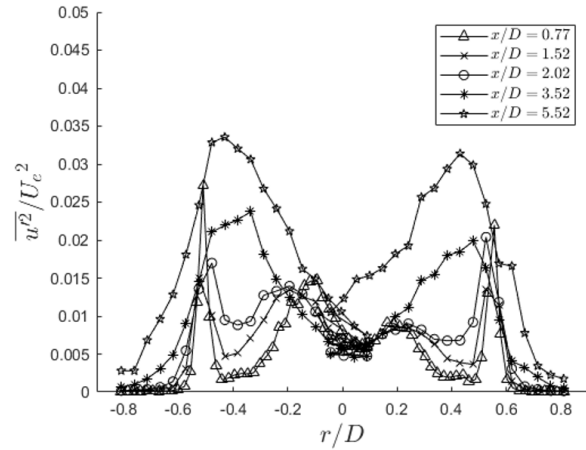
Figure 5. Streamwise velocity variance profile at x/D=0.77 for 2.7×10^6 <$\mathrm{Re_D}$< 7.2×10^6.

Figure 6. Streamwise velocity variance profile at x/D=5.52 for 2.7×10^6 <$\mathrm{Re_D}$< 7.2×10^6.
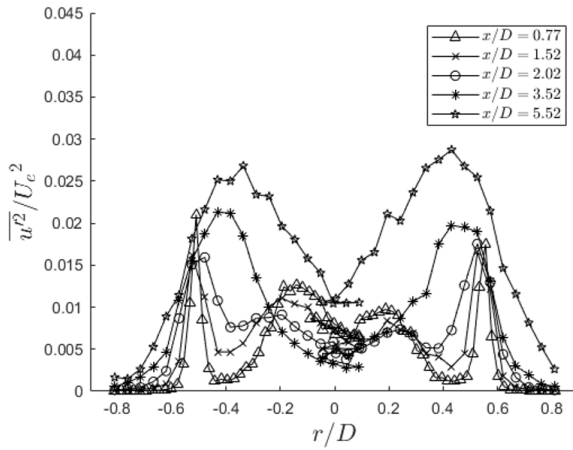
**Figure 7.** Streamwise velocity variance profile evolution at $\mathrm{Re_D}$=2.7×10^6 for 0.77<x/D<5.52.

Figure 8. Streamwise velocity variance profile evolution at $\mathrm{Re_D}$=7.2×10^6 for 0.77<x/D<5.52.

The downstream evolution of the streamwise variance at $\mathrm{Re_D}$ of 2.7×10^6 and 7.2×10^6 can be found in Figures 7 and 8, respectively. As seen for both $\mathrm{Re_D}$ cases, the profile evolves from a multimodal to a bimodal profile shape somewhere in the range 2.02<x/D<3.52. This evolution suggests that the shear layers produced by tip and root vortices evolve and potentially merge to form a single annular shear layer. A similar hypothesis has been suggested in a previous LES study [26]. Before the merger of the two shear layers (x/D< 2.02), the variance peaks associated with the root vortex decrease with increasing downstream distance, suggesting that the root vortex is diffusing faster than the tip vortices. To make stronger conclusions regarding the magnitudes associated with the peaks, such as the asymmetry for both sets of peaks, a higher measurement point density and phase locked statistics are called for in future experiments.

3.3. Power Spectral Density

Power spectral density (PSD) plots were collected using Welch's method through the built in function pwelch in MATLAB. Segment size was equal to a quarter of the sample size with an overlap equal to half of the segment size. Hamming windows were used and were equal in size to the segments. The PSD of the flow near the outer variance peak location is shown in Figure 9. Here the PSD is plotted against the Strouhal number, which is the frequency, f, non-dimensionalized by the freestream velocity and rotor diameter, $St = fD/U_\infty$. A low frequency peak can be observed near $St = 0.3$, and a series of peaks corresponding to harmonics of the turbine's rate of rotation can be seen at higher St. A low frequency peak has been observed in other wake studies, but the Strouhal number varies. In one wind tunnel study, a low frequency behavior was associated with $St = 0.28$ [27] and in another wind tunnel study it was $St = 0.12$ [7]. The low frequency peak is a potential indicator of wake meandering, which has been observed in previous experimental studies [7]. In Figure 9, the green, blue, and red vertical lines represent the first, second, and third harmonics of the turbine's rotation rate, respectively. A dominant signature of the third harmonic was expected, considering the three-bladed turbine used in this study. The high energy peak of the third harmonic is a signature of the tip vortex and has been noted in other experimental wind turbine wake studies [7, 20].
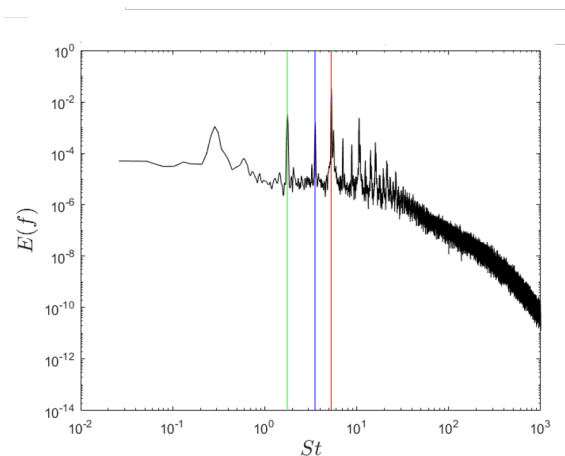
Figure 9. Power spectral density at $\mathrm{Re_D}=2.7\times10^6$ for x/D=0.77 and r/D=0.526. Each colored line represents a different harmonic with respect to the turbine's rotation rate up to the third harmonic.

4. Conclusions

The results from an experimental investigation of the evolution of the wake behind a model HAWT are presented. The experiments were conducted at high Reynolds numbers and wind turbine relevant tip speed ratios, enabled by a unique high-pressure wind tunnel facility. A novel hot-wire anemometer, the NSTAP, was used to obtain well-resolved velocity measurements in the wake. Mean velocity deficit profiles were shown to exhibit a Reynolds number invariant behavior for the entire Reynolds number range tested, agreeing with the findings of canonical axisymmetric wake experiments. Streamwise velocity variance profiles were shown to exhibit a similar Reynolds number invariant behavior, at least close to the rotor. However, neither the mean nor the variance exhibit a self-similar profile, as they are evolving from the rotor influenced state in the near wake towards a far wake behavior. The downstream evolution of the variance profiles reveal the interactions between the tip and root vortices, such as the eventual coalescence of the two distinct shear layers into a single dominating (annular) shear layer. Finally, the PSD

show distinct signatures of the tip vortices, as well as of a lower-frequency structure, indicating a potential signature of the wake-meandering effect.

References

[1] Meneveau C 2019 Big wind power: seven questions for turbulence research *J. of Turbulence* **20** 2–20
[2] Snel H, Schepers J G and Montgomerie B 2007 The MEXICO project (model experiments in controlled conditions): the database and first results of data processing and interpretation *J. Phys.: Conf. Series* **75**
[3] Simms D, Schrek S, Hand M and Fingersh L J 2001 *NREL unsteady aerodynamics experiment in the NASA-Ames wind tunnel: a comparison of predictions to measurements* (Golden, CO: National Renewable Energy Laboratory)
[4] Vermeer L J, Sørensen J N and Crespo A 2003 Wind turbine wake aerodynamics *Progess in Aerospace Sciences* **39** 467–510
[5] Okulov V L and Sørensen J N 2003 Stability of helical tip vortices in a rotor far wake *J. Fluid Mech.* **576** 1–25
[6] Bingöl F, Larsen G C and Mann J 2007 Wake meandering-an analysis of instantaneous 2D laser measurements *J. Physics: Conf. Series* **75**
[7] Medici D and Alfredsson P H 2006 Measurements on a wind turbine wake: 3D effects and bluff body vortex shedding *Wind Energy* **9** 219–36
[8] España G, Aubrun S, Loyer S and Devinant P 2012 Wind tunnel study of the wake meandering downstream of a modelled wind turbine as an effect of large scale turbulent eddies *J. Wind Engineering and Industrial Aerodynamics* **101** 24-33
[9] Chamorro L P, Arndt R E A and Sotiropoulos F 2012 Reynolds number dependence of turbulence statistics in the wake of wind turbines *Wind Energy* **15** 733–42
[10] Micallef D, Ferreira C S, Sant T and van Bussel G 2016 Experimental and numerical investigation of tip vortex generation and evolution of horizontal axis wind turbines *Wind Energy* **19** 1485–501
[11] Miller M A, Kiefer J, Westergaard C, Hansen M O L and Hultmark M 2019 Horizontal axis wind turbine testing at high Reynolds numbers *Phys. Rev. Fluids* **4**
[12] Hansen MOL 1998 *Basic rotor aerodynamics applied to wind turbines* (Technical University of Denmark)
[13] Whale J, Anderson C G, Bareiss R and Wagner S 2000 An exeperimental and numerical study of the vortex structure in the wake of a wind turbine *J. Wind Engineering and Industrial Aerodynamics* **84** 1–21
[14] Vallikivi M, Hultmark M, Bailey S C C and Smits A J 2011 Turbulence measurements in pipe flow using a nano-scale thermal anemometry probe *Exp. Fluids* **51** 1521-7
[15] Townsend A A 1956 *The Structure of Turbulent Shear Flow* (Cambridge University Press)
[16] Jiménez J M, Hultmark M and Smits A J 2010 The intermediate wake of a body of revolution at high Reynolds numbers *J. Fluid Mech.* **659** 516-39
[17] Cannon S C 1991 Large-scale structures and the spatial evolution of wakes behind axisymmetric bluff bodies. Ph.D thesis Department of Aerospace and Mechanical Engineering University of Arizona
[18] Johansson P B V and George W K 2006 The far downstream evolution of the high-Reynolds-number axisymmetric wake behind a disk. Part 1. Single-point statistics *J. Fluid Mech.* 363-85
[19] Bastankhah M and Porté-Agel F 2014 A new analytical model for wind-turbine wakes *Renewable Energy* **70** 116–23
[20] Chamorro L P and Porté-Agel F 2009 A wind-tunnel investigation of wind-turbine wakes: boundary-layer turbulence effects *Boundary-Layer Meteorology* **132** 129–49
[21] Meyers J and Meneveau C 2012 Optimal turbine spacing in fully developed wind farm boundary layers *Wind Energy* **15** 305–17
[22] McTavish S, Feszty D and Nitzsche F 2014 An experimental and computational assessment of blockage effects on wind turbine wake development *Wind Energy* **17** 1515–29
[23] Segalini A and Inghels P 2014 Confinement effects in wind-turbine and propeller measurements *J. Fluid Mech.* **756** 110–29
[24] Sarlak H, Nishino T, Martínez-Tossas L A, Meneveau C and Sørensen J N 2016 Assessment of blockage effects on the wake characteristics and power of wind turbines *Renewable Energy* **93** 340–52
[25] Haans W, Sant T, van Kuik G and van Bussel G HAWT near-wake aerodynamics, Part I: axial flow conditions *Wind Energy* **11** 245–264

[26] Foti D, Yang X, Guala M and Sotiropoulos F 2016 Wake meandering statistics of a model wind turbine: insights gained by large eddy simulations *Phys. Rev. Fluids* **1**

[27] Chamorro L P, Hill C, Morton C, Ellis C, Arndt R E A and Sotiropoulos F On the interaction between a turbulent open channel flow and an axial-flow turbine *J. Fluid Mech.* **716** 658-670